Shear wave elastography of placenta: *in vivo* quantitation of placental elasticity in preeclampsia

Fahrettin Kılıç, Yasemin Kayadibi, Mehmet Aytaç Yüksel, İbrahim Adaletli, Fethi Emre Ustabaşıoğlu, Mahmut Öncül, Rıza Madazlı, Mehmet Halit Yılmaz, İsmail Mihmanlı, Fatih Kantarcı

PURPOSE
We aimed to evaluate the utility of shear wave elastography (SWE) for assessing the placenta in preeclampsia disease.

METHODS
A total of 50 pregnant women in the second or third trimester (23 preeclampsia patients and 27 healthy control subjects) were enrolled in the study. Obstetrical grayscale and Doppler ultrasonography, SWE findings of placenta, and prenatal/postnatal clinical data were analyzed and the best SWE cutoff value which represents the diagnosis of preeclampsia was determined. Sensitivity, specificity, positive predictive value (PPV), negative predictive value (NPV), and diagnostic accuracy of preeclampsia were calculated based on SWE measurements.

RESULTS
Mean stiffness values were much higher in preeclamptic placentas in all regions and layers than in normal controls. The most significant difference was observed in the central placental area facing the fetus where the umbilical cord inserts, with a median of 21 kPa (range, 3–71 kPa) for preeclampsia and 4 kPa (range, 1.5–14 kPa) for the control group (P < 0.01). The SWE data showed a moderate correlation with the uterine artery resistivity and pulsatility indices. The cutoff value maximizing the accuracy of diagnosis was 7.35 kPa (area under curve, 0.895; 95% confidence interval, 0.791–0.998); sensitivity, specificity, PPV, NPV, and accuracy were 90%, 86%, 82%, 92%, and 88%, respectively.

CONCLUSION
Stiffness of the placenta is significantly higher in patients with preeclampsia. SWE appears to be an assistive diagnostic technique for placenta evaluation in preeclampsia.

Preeclampsia is one of the leading causes of maternal and perinatal morbidity and mortality, with preterm delivery occurring in approximately 5%–8% and perinatal mortality occurring in 1%–3% of pregnancies, worldwide (1). Common maternal complications of severe preeclampsia can include disseminated coagulopathy/HELLP syndrome, pulmonary edema, acute renal failure, placenta abruption, and long-term cardiovascular complications (2, 3). Common fetal complications are fetal growth restriction, preterm delivery, and perinatal death (4).

The elasticity term defines the continuum mechanics of bodies that deform reversibly under strain. Shear wave elastography (SWE) is a novel ultrasonography (US) technique which is used to obtain elasticity information that represents the constituent of soft tissues. The principle of the modality is based on inducing mechanical vibration using acoustic radiation force, gathering the transverse shear waves that propagate laterally away from the tissue, and calculating their velocity. This kinetic method provides real-time quantitative data and has high reproducibility without compression effects/artifacts, as well as a deeper tissue response compared to static elastography (5, 6). We hypothesized that using noninvasive SWE to identify global structural disorganization of the placenta due to preeclampsia pathogenesis would help to detect the disease. To the best of our knowledge, the application of SWE for placental evaluation in preeclampsia has not been studied previously. In the present study, we inspected the SWE values related to changes in placental elasticity in preeclampsia and determined its utility for assessing the disease.

Methods

This study was conducted at Istanbul University Cerrahpasa School of Medicine between January and June 2013. The study was approved by the internal review board and was designed in accordance with the Declaration of Helsinki. Written informed consent was obtained from all patients who participated in the study. A total of 50 singleton pregnant women in the second or third trimester were enrolled. The participants included 23 consecutive pregnant women diagnosed with preeclampsia and 27 healthy consecutive age-matched pregnant women who had no risk factors for the diagnosis of preeclampsia. Mean age was 33.5±5.3 years (range, 22–45 years) in preeclampsia group and 33.3±4.69 years (range, 26–42 years) in healthy controls. Pregnant women with placental anomalies as well as insufficient placental adherence or penetration, misdevelopment, and complications including hematoma and gross calcifications were excluded from the study. Also excluded were women with multiple gestations, pregnancies with fetal chromosomal or major

From the Department of Radiology (F.K. ✉ *fahrettinkilic@hotmail.com*, Y.K., İ.A., Y.E.U., M.H.Y., İ.M., F.K.), the Department of Obstetrics and Gynecology (M.A.Y., M.Ö., R.M.) Istanbul University Cerrahpasa School of Medicine, Istanbul, Turkey.

structural anomalies, miscarriage history, severe anemia (hemoglobin <6 g/dL), patients with accompanying disease(s), and those with a posterior placental location in the uterus to avoid inadequate elasticity calculations.

Demographic characteristics, detailed medical and obstetrical data, and prenatal care charts were examined. Postnatal findings such as birth weight, Apgar scores at first and fifth minutes, and short-term medical conditions were collected. Preeclampsia was diagnosed according to the criteria of the American College of Obstetricians and Gynecologists (7). Preeclampsia was defined and diagnosed as the onset of hypertension (systolic to diastolic blood pressure ≥140/90 mm Hg) and proteinuria (>300 mg/day in 24-hour urine collection or protein concentration of 1 g/L) during the pregnancy with both conditions remitting after delivery.

Imaging technique

The grayscale, Doppler, and elastography time scales of the US examination were shortened to minimize sound wave exposure. Grayscale and color Doppler US exams were performed by an obstetrician with more than 20 years of experience (R.M.) and SWE examinations were performed by a radiologist with more than seven years of experience with US and three years of experience with elastography (F.K.). Grayscale and Doppler examinations were performed using Ultramark 9 (Advanced Technologies Laboratory) with a 3.5 MHz color-pulsed Doppler. Gestational age was determined based on the last normal menstrual period and according to the crown–rump length on the first trimester US exam. The largest vertical pocket of amniotic fluid was measured and <2 cm was labeled as oligohydramnios. After evaluating the biophysical profile with US, abdominal subcutaneous fat thickness, placental thickness, morphology, and relation to uterus were noted. Doppler velocimetry was applied to both uterine arteries in three consecutive waveforms; the diastolic notch presence was investigated, and resistivity index (RI), pulsatility index (PI), peak systolic, and end diastolic velocity ratios were measured. Doppler US was applied with the sampling gate set at 2 mm and the angle of implementation less than 60°.

All SWE examinations were performed with a 1–6 MHz curved array transducer (Aixplorer, SuperSonic Imagine). Before starting the study, 10 healthy pregnant women were examined for standardization of the elastography technique. The radiologist who applied SWE was blinded to the US and Doppler imaging findings and patient histories. Elastography examination was performed with the patient lying in the supine position. Sagittal imaging planes were used to obtain a perpendicular view of the nearest region of the placenta. Imaging plane was limited to superficial view to prevent deeper beam penetration over fetus and besides, the imaging focus was elevated over placenta in each grayscale and elastography imaging. Excessive transmission gel was used to eliminate any compression artifact of the probe. During acquisitions, patients were asked to breathe lightly and refrain from moving. Thermal and mechanical indices were noted for each examination.

The machine software displays elastograms as an overlay in dual mode (vertical/horizontal) simultaneously with grayscale images to aid the morphological correlation of the placenta. A rectangular adjustable inner image box, which is included with the system software, was used for SWE examination. This inner box displays the real-time stiffness on a chromatic scale with a spectrum from blue to red indicating the shear intensity (stiffness). The upper threshold of the spectral scale can be adjusted manually and the changes do not affect the measured shear intensity value. The spectral color-coding box on the image allows the region of interest (ROI) to be placed in the area where the greatest stiffness is observed. After freezing the elastography image, software allows the operator to place a circular ROI of various diameters within the elastography window. Color-saturated images were used to perform calculations. In the present study, the ROI sizes were fixed to 5 mm in all cases. Tissue elasticity was measured in kilopascals (kPa) of the spectrum scale, which guided the placement of the ROI cursor. The US image window was narrowed to obtain adequate image quality and more precise elasticity calculations. After the display image was frozen, minimum, maximum, and mean elasticity of four samples from fetal and maternal surfaces in the peripheral and central regions of the placenta were calculated using the ROI.

Statistical analysis

Statistical analyses were performed using the SPSS software (version 16.0, SPSS Inc.). The maximum and mean elasticity within the ROI were expressed as the mean of three different measurements. Kolmogorov-Smirnov test was used to analyze the normal distribution of data. Differences in age, gestational age, placental thickness, subcutaneous fat thickness, birth weight, Apgar scores, Doppler indices, presence of a diastolic notch, and shear elastic modulus data of the placenta between patients with and without preeclampsia were evaluated using the Mann-Whitney U test. All measurements were expressed as medians. All of the SWE data were correlated to Doppler indices using the Pearson correlation test. A $P < 0.05$ was considered as statistically significant. Receiver-operating characteristic curves were plotted to check the discriminatory power of each group, and the best SWE cutoff value which represents the diagnosis of preeclampsia was determined by the Youden index (J). Sensitivity, specificity, positive predictive value (PPV), negative predictive value (NPV), and accuracy were calculated based on SWE measurements.

Results

Table 1 presents clinical scores including age, gestation age during application of SWE, birth weights and Apgar scores, placental and subcutaneous fat thickness, and Doppler indices of the preeclampsia and control groups. The mean age was not significantly different between the two groups. Gestational age at evaluation ranged from 27 to 37 weeks (median, 34 weeks) in the control group and 23 to 35 weeks (median, 28 weeks) in the preeclampsia group. There was a slight

Table 1. Medical and obstetric characteristics of women with preeclampsia and healthy controls

	Preeclampsia (n=23)			Control (n=27)			
	Median	Min	Max	Median	Min	Max	P
Age (year)	34	22	45	34	26	42	0.815
Gestational age (week)	28	23	35	30	27	37	0.016
Birth weight (g)	1220	290	3580	3500	1700	4520	<0.001
APGAR score, 1 min	6	0	8	8	6	9	<0.001
APGAR score, 5 min	7	0	9	9	5	10	<0.001
Subcutaneous fat thickness (mm)	30	10	50	25	5	50	0.014
Placental thickness (mm)	39	22	69	39	29	61	0.953
Right UA PI	1.36	0.36	2.33	0.6	0.18	1.52	<0.001
Left UA PI	1.24	0.38	2.50	0.65	0.27	1.31	<0.001
Right UA RI	0.71	0.30	0.90	0.54	0.23	1.14	<0.001
Left UA RI	0.76	0.31	0.90	0.54	0.27	0.79	<0.001

Data are presented as median, minimum, and maximum.
Min, minimum; max, maximum; UA, uterine artery; PI, pulsatility index; RI, Resistivity index.

difference in gestation age between the control and the preeclampsia groups ($P < 0.05$). The median birth weight was significantly higher in the control group (3500 g; range, 1700–4520 g) than in the preeclampsia group (1220 g; range, 290–3580 g) ($P < 0.001$). Preeclampsia had a notable impact on fetal Apgar scores. Control group had higher 1 min and 5 min Apgar scores than the preeclampsia group (1 min: 8 vs. 6; 5 min: 9 vs. 7; $P < 0.001$, for both). The change in Apgar scores from 1 min to 5 min was not significantly different in either group ($P > 0.05$). Intrauterine survival rates were better in the control group ($P < 0.05$). Overall, three pregnancies in the preeclampsia group ended with intrauterine death; however, no similar cases occurred in the control group.

The median placental thickness was 39 mm (range, 22–69 mm) in the normal group and 39 mm (range, 29–61 mm) in the preeclampsia group. Table 1 presents the radiological scores of Doppler US as well as the RI and PI of the bilateral uterine artery. A diastolic notch was present in 56.5% (13/23) of the preeclampsia cases and none of the healthy controls. The median RI and PI of the right and left uterine arteries in the preeclampsia group were significantly higher than the relevant indices in the control group. The median RI for the right and left uterine arteries were 0.71 and 0.76 respectively, in the preeclampsia group and 0.54 for both the right and left uterine arteries in the control group ($P < 0.001$, for both). The median PI of the right and left uterine arteries was 1.36 and 1.24, respectively, in the preeclampsia group and 0.6 and 0.65, respectively, in the control group ($P < 0.001$, for both). The mean PI of fetal umbilical artery was significantly higher in the preeclampsia group (1.17±0.5 vs. 0.81±0.15, $P < 0.001$), while the RI of fetal umbilical artery did not differ between the groups (0.69±0.12 vs. 0.63±0.08, $P > 0.05$).

SWE radiological scores are presented in Table 2. Elasticity values were determined from four different areas: the peripheral edge and central region of the placenta from the fetal and maternal surfaces. The mean stiffness values were much higher in preeclamptic placentas in all regions and layers than in normal controls (Fig. 1). The most significant difference was observed in the kPa values of the central placental area facing the fetus where the umbilical cord inserts with a median of 21 kPa (range, 3–71 kPa) for the preeclampsia group and 4 kPa (range, 1.5–14 kPa) for the healthy control group ($P < 0.001$). The SWE data was moderately correlated with the uterine artery PI and weakly correlated with the uterine artery RI (Table 3).

The maximum area under the curve (AUC) for the diagnosis of preeclampsia is based on median elasticity values acquired from the central placental area facing the fetus (Fig. 2). The cutoff value maximizing the accuracy of diagnosis was 7.35 kPa (AUC, 0.895; 95% confidence interval, 0.791–0.998); sensitivity, specificity, PPV, NPV, and diagnostic accuracy of this cutoff value were 90%, 86%, 82%, 92%, and 88%, respectively.

Thermal and mechanical indices of elastography examination were within the safety limits for fetal evaluation. The mean mechanical index was 1.3±0.12 (1.1–1.5) for the control group and 1.28±0.12 (1.1–1.5) for preeclampsia patients. The mean thermal index was 1.63±0.08 (1.4–1.7) for the control group and 1.62±0.11 (1.3–1.7) for preeclampsia patients.

Discussion

Our SWE results showed significantly higher placental stiffness in preeclampsia patients. Associated factors affecting the fetus were also found among preeclampsia patients, such as low birth weight, low Apgar scores, and Doppler US results that were compatible with well-known diagnostic performances.

Elasticity imaging has been clinically used for more than 10 years with recent improvements such as shear wave imaging technology. SWE revealed that malignant tissues of breast lesions have higher stiffness due to the increase in the number of malignant cells and surrounding desmoplas-

Table 2. Medical and obstetric characteristics of women diagnosed with preeclampsia and healthy controls

Elastography region of interest	Preeclampsia (n=23)			Control (n=27)			
	Median	Min	Max	Median	Min	Max	P
Central-maternal surface of the placenta							
Mean elastic modulus (kPa)	25	2.4	66.5	5.8	2.5	13	< 0.001
Max elastic modulus (kPa)	30	3	70	9	2.8	21.4	<0.001
Central-fetal surface of the placenta							
Mean elastic modulus (kPa)	21	3	71	4	1.5	14	<0.001
Max elastic modulus (kPa)	28	3.7	98	5.8	2	21.6	<0.001
Peripheral-maternal surface of the placenta							
Mean elastic modulus (kPa)	19	3	67	5	1.8	14.7	<0.001
Max elastic modulus (kPa)	31	3.5	93	7.1	4.6	23	<0.001
Peripheral-fetal surface of the placenta							
Mean elastic modulus (kPa)	14	2.6	60	5.2	1.6	14	<0.001
Max elastic modulus (kPa)	17	3.8	87	6	2.9	18	<0.001

Data are presented as median, minimum, and maximum.
Min, minimum; max, maximum; kPa, kilopascals.

Table 3. Correlation of median elasticity values of the central-fetal surface of the placenta, by uterine artery Doppler US

	Right UA PI	Left UA PI	Right UA RI	Left UA RI
r	0.512	0.436	0.295	0.339
P	0.000	0.002	0.038	0.016

UA, uterine artery; PI, pulsatility index; RI, resistivity index.

tic reactions (8). Several studies have evaluated noninvasive elastographic techniques for assessing liver fibrosis, which may decrease the need for liver biopsy (9). Other organ systems such as the hormone secretion system and the musculoskeletal system (10) have also been investigated.

Placenta was evaluated by sonoelastography in recent studies. Our study shows that elasticity samples taken from different areas of the placenta differ in preeclampsia with the center of the umbilical cord insertion area being the most significant, suggesting that the disease may predominantly affect the central region of the placenta. In contrast, elasticity in normal placentas does not differ among various regions. Our results for the control group were in agreement with the results of Li et al. (11). Our results are also compatible with a recent study on postpartum placentas, which reported higher elasticity values in the central region of the placenta of intrauterine growth-restricted

fetuses and hypertensive pregnancies (12). Their elasticity values cannot be compared to ours due to their *ex vivo* study design. However, they did inspect placentas from pregnancies with fetal growth restrictions and reported that the cause of elasticity increase is due to histological changes of widespread infarction and inflammation.

We found that the most significant mean stiffness value for diagnosis of preeclampsia was 7.35 kPa, with 90% sensitivity and 86% specificity. Diastolic notches were not detected in the healthy control group, and had a specificity of 100%. However, the presence of diastolic notch in the patient group led to a sensitivity of 56.5%. Supplemental analysis using 7.35 kPa cutoff value with presence of diastolic notch indicated sensitivity, specificity, PPV, and NPV rates as 91.3%, 92.6%, 91.3%, and 92.6%, respectively. Besides, increase of the Doppler indices of uterine arteries in preeclampsia group were moderately correlated with increase of

elasticity values of placenta, as well as the pulsatility indices of umbilical artery which reflects the fetal well-being. Real-time *in vivo* SWE demonstrated increase in stiffness, which indirectly reflects the deterioration of placenta in preeclampsia disease.

Preeclampsia may occur for different reasons and the pathophysiology leading to disease onset may differ before 34 weeks of gestation, at term, during labor, and postpartum (13). Impaired uteroplacental blood flow results in disruption of inflammatory cytokine regulation, bioactivation of relaxin, and activation of the renin-angiotensin system, which are suggested mechanisms of hypertension in preeclampsia (14). When considering the structural causality of these biochemical changes, the first stage in the development of preeclampsia is inadequate placental cytotrophoblast invasion, trophoblast invasion, and maternal spiral artery remodeling (15). Eventually, the unsuccessful trophoblast invasion of the muscular spiral arteries into the myometrial layer and transformation of these "low-resistance" capacitance vessels result in placental ischemia and hypoxia. These preeclamptic disturbances can eventually cause excessive syncytial knots, infarcts covering more than 10% of the placental area, decidual vasculopathy, absence of intermediate villi, and placental erythroblastosis (16).
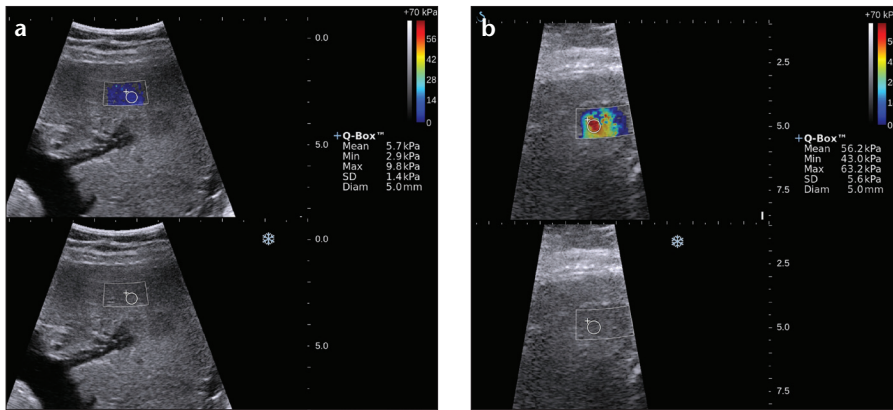
Figure 1. a, b. Shear wave elastography (SWE) images of placenta in pregnant women with and without preeclampsia. The sagittal imaging plane **(a)** shows the placenta of a 23-year-old pregnant woman in the 32nd week of gestation with no findings of preeclampsia. Two split US and shear wave elastography images are at the same level. The rectangular box represents the stiffness in blue and ROI is placed in the denser area. Mean and maximum elasticity was measured as 5.7 kPa and 9.8 kPa, respectively. Panel **(b)** shows the SWE image of a 30-year-old preeclampsia patient in the 28th week of gestation. The rectangular box represents the stiffness spectrum in blue to red. ROI is placed in peak stiffness area which is represented in red. Mean and maximum elasticity was measured as 56.2 kPa and 63.2 kPa, respectively.
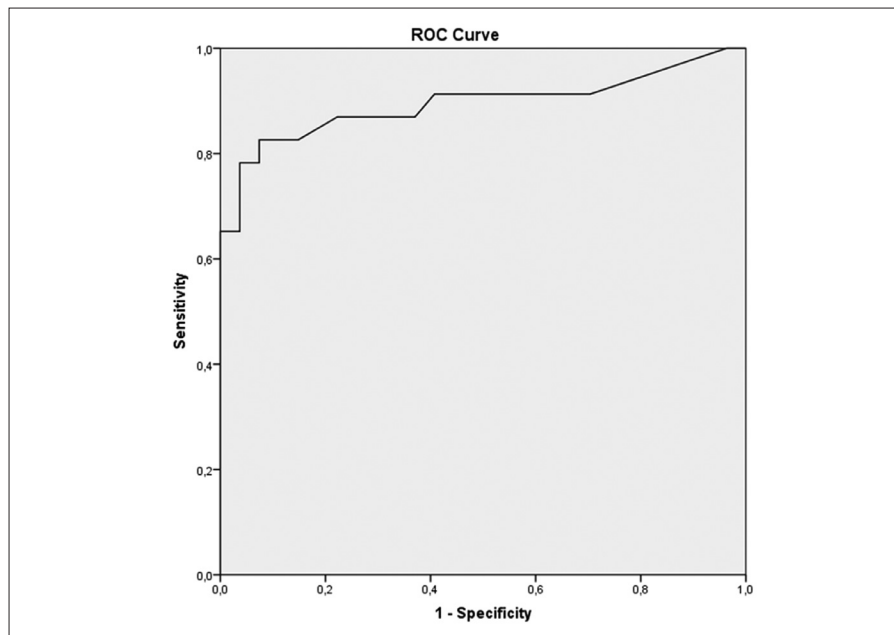
Figure 2. The receiver operating characteristic (ROC) curve for median stiffness value at the central fetal surface of the placenta (n=50).

Trophoblastic ischemia or hypoxia counteracts syncytial hyperplasia and syncytial knots form as the focal aggregation or clumping of syncytial nuclei on the outer surface of the tertiary placental villous (17). Hottor et al. (18) suggested that there is an inverse relationship between the proportions of fibrin and anchoring villi. Increased deposition of fibrin and reduced materno-fetal anchoring area are seen in preeclampsia. On the other hand, Devisme et al. (16) observed intervillous fibrin deposition in preeclampsia, but did not find a statistically significant difference compared with normal placenta. Hence, stiffness increases detected by SWE should mainly be due to vasculopathy, inflammation, fibrin deposition, and excessive syncytial knots.

From the biochemical and histological perspective, only *ex vivo* methods can be used to investigate histopathological structure. *In vivo* examination is not feasible because of placental vulnerability during tissue sampling. Imaging techniques are extensively used to investigate placental morphology and function. Conventional B-mode US can provide information on the overall appearance and location of the placenta, but not on function. Doppler US is an accepted imaging method that has been used extensively. The method inspects the presence of diastolic notches and the PI increase of uterine arteries in the second trimester of pregnancies that are known to be at risk for developing preeclampsia (19). A previous multivariate logistic regression analysis determined that abnormal uterine artery Doppler findings are independent markers for patients at increased risk of developing early-onset preeclampsia at less than 34 weeks of gestation (19).

An important touchstone is the safety issue. Pregnant women undergo repeated US examinations during pregnancy. The teratogenous effect of ultrasound exposure has been extensively studied by several researchers for decades (20). In the first eight weeks of pregnancy, it is advised to avoid longer sound wave exposure due to teratogenic exposure. This exposure is defined by thermal and mechanical indices which depends on ultrasound frequency, focusing, and duration of exposure. Care should be taken to adjust these parameters for lower exposure. Fetal exposure to ultrasound is limited by the US Food and Drug Administration (FDA) to a maximum spatial peak temporal average intensity of 720 mW/cm and maximum mechanical index of 1.9 (21). British Medical Ultrasound Society handles the thermal effect by means of duration of exposure (22). The thermal index of our study (mean, 1.6) is advised for no more than 15 minutes and covers the safety limits of the study. The elastography device's acoustic output, mechanical and thermal indices in the present study are within the established safety ranges. Sugitani et al. (12) investigated the biological effects of acoustic radiation force impulse imaging on full-term delivered placentas and did not recover any thermal or mechanical structural changes. Tabaru et al. (23) investigated the thermal effect of acoustic radiation force elastography and suggested that high intensity US could be used

for fetal examination because amnion liquid has no ultrasonic attenuation and does not transmit push wave. We aimed to use elastography in shortest duration possible, particularly for superficial imaging of the placenta.

Our study has several limitations. We could not determine the diagnostic efficiency of the technique in different stages of preeclampsia or complications due to lack of an adequate number of patients. Another limitation of our study is the absence of histopathological evaluation of the placentas. Histopathological examination may show a relationship between structural changes in the pathology and elastography findings. Although the standardization of the elastography technique was satisfactory, we did not evaluate interobserver variability because we aimed to minimize repeated examinations of the same fetus. There was a slight difference between the control and the preeclampsia groups in gestation age because of randomized inclusion of cases in the study series. There is no study in the literature showing the relationship between elasticity of the placenta and gestational age. Further correlative studies of the placenta are necessary to determine elasticity of the placenta with respect to the gestational age.

In conclusion, we have demonstrated the diagnostic application of SWE imaging to preeclampsia. This is the first report on the *in vivo* quantitation of placental elasticity in preeclampsia. Real-time demonstrations of elasticity changes may indirectly manifest structural deterioration before clinical presentation of the preeclampsia disease occurs. Future studies involving early pregnancies and a larger number of patients with preeclampsia may confirm the usefulness of SWE imaging for predicting preeclampsia.

Conflict of interest disclosure

The authors declared no conflicts of interest.

References

1. Xiong X, Buekens P, Pridjian G, Fraser WD. Pregnancy-induced hypertension and perinatal mortality. J Reprod Med 2007; 52:402–406.
2. Brown MC, Best KE, Pearce MS, Waugh J, Robson SC, Bell R. Cardiovascular disease risk in women with pre-eclampsia: systematic review and meta-analysis. Eur J Epidemiol 2013; 28:1–19. [CrossRef]
3. Kuklina EV, Ayala C, Callaghan WM. Hypertensive disorders and severe obstetric morbidity in the United States. Obstet Gynecol 2009; 113:1299–1306. [CrossRef]
4. Gupta LM, Gaston L, Chauhan SP. Detection of fetal growth restriction with preterm severe preeclampsia: experience at two tertiary centers. Am J Perinatol 2008; 25:247–249. [CrossRef]
5. Cosgrove DO, Berg WA, Dore CJ, et al. Shear wave elastography for breast masses is highly reproducible. Eur Radiol 2012; 22:1023–1032. [CrossRef]
6. Evans A, Whelehan P, Thomson K, et al. Quantitative shear wave ultrasound elastography: initial experience in solid breast masses. Breast Cancer Res 2010; 12:R104. [CrossRef]
7. ACOG practice bulletin. Diagnosis and management of preeclampsia and eclampsia. Number 33, January 2002. Obstet Gynecol 2002; 99:159–167.
8. Berg WA, Cosgrove DO, Dore CJ, et al. Shear-wave elastography improves the specificity of breast US: the BE1 multinational study of 939 masses. Radiology 2012; 262:435–449. [CrossRef]
9. Frulio N, Trillaud H. Ultrasound elastography in liver. Diagn Interv Imaging 2013; 94:515–534. [CrossRef]
10. Botanlioglu H, Kantarci F, Kaynak G, et al. Shear wave elastography properties of vastus lateralis and vastus medialis obliquus muscles in normal subjects and female patients with patellofemoral pain syndrome. Skeletal Radiol 2013; 42:659–666. [CrossRef]
11. Li WJ, Wei ZT, Yan RL, Zhang YL. Detection of placenta elasticity modulus by quantitative real-time shear wave imaging. Clin Exp Obstet Gynecol 2012; 39:470–473.
12. Sugitani M, Fujita Y, Yumoto Y, et al. A new method for measurement of placental elasticity: Acoustic radiation force impulse imaging. Placenta 2013; 34:1009–1013. [CrossRef]
13. Dekker G, Sibai B. Primary, secondary, and tertiary prevention of pre-eclampsia. Lancet 2001; 357:209–215. [CrossRef]
14. Sibai B, Dekker G, Kupferminc M. Pre-eclampsia. Lancet 2005; 365:785–799. [CrossRef]
15. Pijnenborg R, Vercruysse L, Hanssens M. The uterine spiral arteries in human pregnancy: facts and controversies. Placenta 2006; 27:939–958. [CrossRef]
16. Devisme L, Merlot B, Ego A, Houfflin-Debarge V, Deruelle P, Subtil D. A case-control study of placental lesions associated with pre-eclampsia. Int J Gyneacol Obstet 2013; 120:165–168. [CrossRef]
17. Baergen RN. Manual of Benirschke and Kaufmann's pathology of the human placenta. 2nd ed. New York: Springer Science & Business Media, 2005; 72–74.
18. Hottor B, Bosio P, Waugh J, et al. Variation in composition of the intervillous space lining in term placentas of mothers with pre-eclampsia. Placenta 2010; 31:409–417. [CrossRef]
19. Espinoza J, Kusanovic JP, Bahado-Singh R, et al. Should bilateral uterine artery notching be used in the risk assessment for preeclampsia, small-for-gestational-age, and gestational hypertension? J Ultrasound Med 2010; 29:1103–1115. [CrossRef]
20. Consensus Conference: The use of diagnostic ultrasound imaging during pregnancy. JAMA 1984; 252:669–672. [CrossRef]
21. Nyborg WL. Biological effects of ultrasound: development of safety guidelines. Part I: personal histories. Ultrasound Med Biol 2000; 26:911–964. [CrossRef]
22. Safety Group of th e British Medical Ultrasound Society. Guidelines for the safe use of diagnostic ultrasound equipment. Ultrasound 2010; 18:52–59. [CrossRef]
23. Tabaru M, Yoshikawa H, Azuma T, Asami R, Hashiba K. Experimental study on temperature rise of acoustic radiation force elastography. J Med Ultrasonics 2012; 39:137–146. [CrossRef]